Am J Cancer Res 2023;13(12):6011-6025
www.ajcr.us /ISSN:2156-6976/ajcr0153755

Original Article

Induction of resistance to oxaliplatin in cancer by a microRNA/Fem1B/Gli1 pathway

Yi-Chen Su[1,2,8], Landon Tyler Metzen[1], Leandro Martín Vélez[1], Elodie Bournique[1], Marcus Seldin[1], Rémi Buisson[1], Wei-Wen Kuo[3], Chih-Yang Huang[2,4,5,6,7,8], Peter Kaiser[1]

[1]Department of Biological Chemistry, University of California, Irvine, California 92697, USA; [2]Graduate Institute of Basic Medical Science, China Medical University, Taichung 404, Taiwan; [3]Department of Biological Science and Technology, China Medical University, Taichung 404, Taiwan; [4]Cardiovascular and Mitochondrial Related Disease Research Center, Hualien Tzu Chi Hospital, Buddhist Tzu Chi Medical Foundation, Hualien 970, Taiwan; [5]Center of General Education, Buddhist Tzu Chi Medical Foundation, Tzu Chi University of Science and Technology, Hualien 970, Taiwan; [6]Department of Medical Research, China Medical University Hospital, China Medical University, Taichung 404, Taiwan; [7]Department of Medical Laboratory Science and Biotechnology, Asia University, Taichung 413, Taiwan; [8]Graduate Institute of Biomedical Sciences, China Medical University, Taichung 404, Taiwan

Received October 3, 2023; Accepted November 21, 2023; Epub December 15, 2023; Published December 30, 2023

Abstract: Colorectal cancer is among the most common cancers worldwide and a frequent cause of cancer related deaths. Oxaliplatin is the first line chemotherapeutics for treatment, but the development of resistance leads to recurrence of oxaliplatin insensitive tumors. To understand possible mechanisms of drug tolerance we developed oxaliplatin resistant derivatives (OR-LoVo) of the established LoVo cell line originally isolated from a metastatic colon adenocarcinoma. We compared the microRNA (miRNA) expression profile of the cell pair and found expression of miR-29a-3p significantly increased in OR-LoVo cells compared to parent cells. In addition, miR-29a-3p was significantly elevated in tumor tissue when compared to matched surrounding tissue in human, suggesting potential clinical importance. Ectopic miR-29-a-3p expression induced chemoresistance in a number of different cancer cell lines as well as colorectal tumors in mice. We further demonstrated that miR-29-a-3p downregulates expression of the ubiquitin ligase component FEM1B and that reduction of Fem1b levels is sufficient to confer oxaliplatin resistance. FEM1B targets the glioma associated oncogene Gli1 for degradation, suggesting that increased Gli1 levels could contribute to oxaliplatin tolerance. Accordingly, knockdown of GLI1 reverted chemoresistance of OR-LoVo cells. Mechanistically, resistant cells experienced significantly lower DNA damage upon oxaliplatin treatment, which can be partially explained by reduced oxaliplatin uptake and enhanced repair. These results suggest that miR-29-a-3p overexpression induces oxaliplatin resistance through misregulation of Fem1B and Gli1 levels. TCGA analyses provides strong evidence that the reported findings regarding induced drug tolerance by the miR-29a/Fem1B axis is clinically relevant. The reported findings can help to predict oxaliplatin sensitivity and resistance of colorectal tumors.

Keywords: Drug-resistance mechanism, oxaliplatin, microRNAs, DNA damage, fem-1 homolog B (Fem1B), glioma-associated oncogene homolog 1 (Gli1)

Introduction

Colon cancer is the third most frequent cause of death and remains a great health problem despite screening for early detection of lesions [1]. Oxaliplatin is commonly used for the treatment of colorectal carcinoma [2, 3]. The antineoplastic activity of oxaliplatin is caused by formation of covalent adducts with DNA, which prevents DNA replication and transcription, and ultimately induces cell death [4]. The introduction of oxaliplatin for treatment of colorectal cancer in 2000 resulted in increased overall patient survival. However, despite good response rates, development of drug resistance followed by recurrence of tumors is a significant problem that leads to treatment failure. Understanding resistance mechanisms and identification of markers of resistance is therefore an important goal to improve treatment decisions and outcome. Resistance to oxaliplatin can be caused by increased drug efflux or

metabolism, altered DNA repair efficiency, and changes in the apoptotic as well as necrotic response [5].

In an effort to evaluate the contribution of miRNAs to oxaliplatin resistance in colorectal cancer, we used a previously developed cell model based on LoVo cells, which were developed from a metastatic colon adenocarcinoma. Oxaliplatin resistant-LoVo (OR-LoVo) cells were isolated by successive treatment of the parent cells with oxaliplatin in tissue culture. This cell pair was profiled for miRNA expression in previous work and differential regulation of miR-31-5p, miR-100-5p, and miR-29a-3p was detected [1]. In this study we focused on miR-29a-3p. A predicted target of miR-29a-3p is the evolutionary conserved VHL-box protein Fem1B [6]. Fem1B is a substrate recognition subunit of the Cul2-ubiquitin ligase and has been shown to target stem-loop binding protein (SLBP) and the Glioma-Associated Oncogene Homolog 1 (GLI1) for degradation by the 26S proteasome in humans [6]. Fem1B is a proapoptotic protein and its levels have been linked to regulation of apoptosis in colon cancer cells [7, 8]. More recently, the ubiquitin ligase $Cul2^{Fem1B}$ and its substrate Fnip1were identified as the core component that coordinates reductive stress response [9, 10]. Here, we show that increased expression of miR-29a-3p reduces Fem1b levels to mediate resistance to oxaliplatin treatment in colon cancer cells and tumor models.

Materials and methods

Cell culture

LoVo cells were acquired from Bioresource Collection and Research Center (Hsinchu, Taiwan) and were cultured in RPMI 1640 medium (Gibco, Carlsbad, CA, USA) with 10% heat-inactivated fetal bovine serum (FBS; HyClone, Utah, USA) in humidified air with 5% CO_2 at 37°C. Cell culture medium was replaced with fresh media 48 h after sub-culturing. An aliquot of 3.5 mL Dulbecco's phosphate-buffered saline (PBS; GIBCO, Auckland, New Zealand) was used to wash each 10-cm culture plate. Finally, fresh RPMI 1640 was placed in each culture plate (10 mL/plate).

For selection of oxaliplatin resistant cells (OR-LoVo) 10^6 LoVo cells were incubated for 12 h before oxaliplatin was added to a final concentration of 15 μM, the determined IC_{50} for parental cells, for 48 h. The IC_{50} for the pool of surviving cells was then determined (=IC_{50} [2]) using an MTT assay. Cells were then plated at 70% confluency and cultured for 12 h before a second selection with oxaliplatin for 48 h. The oxaliplatin concentration was increased to the determine IC_{50} [2]. Surviving cells were reseeded three times at 70% confluency and selected with oxaliplatin for 24 h each cycle. Oxaliplatin was used at the IC_{50} [2] concentration. Surviving cells were then cultured in 25 μM oxaliplatin until no cell death was observed. The surviving cell population was used as OR-LoVo.

CRISPR-knockout

The lentiCRISPR v2 plasmid (Addgene #52961) [11] was used to knockout mir-29a-3p. Target sequences were selected using CRISPR DESIGN (http://crispr.mit.edu/) [12]. The vector was digested by using BsmBI (New England Biolabs), and a pair of annealed oligos was cloned into the single guide RNA scaffold. The following sequence was used sgRNA mir-29a-3p: 5'-TAGCACCATCTGAAATCGGTTA-3'. CRISPR/cas9 constructs were transfected into cells with the BioT reagent (Bioland Scientific LLC), treated with puromycin (Life Technologies) to select knockout cell lines, and confirmed by Western blot.

Lentivirus shRNA knockdown and overexpression

pSLIK-Hygro and pEN_TmiRc3 plasmids (Addgene #25737 and #25748) [13] were used for inducible expression of miR-29a-3p, and shRNAs against FEM1B and GLI1. Human FEM1B (shRNA), 5'-agcgCGCGGATAATATGGAATTTGAGTAGTGAAGCCACAGATGTACTCAAATTCCATATTATCCGCAtgcc-3'; human GLI1 (shRNA), 5'-agcgAAGCCTGAATCTGTGTATGAAATAGTGAAGCCACAGATGTATTTCATACACAGATTCAGGCTCtgcc-3'. Sequences were designed with design BfuAI compatible protrusions (lower cased) for cloning into the BfuAI site in pEN_TGmirRc3. The pSLIK lentiviral construct was then generated and used to develop stable cell lines with inducible expression of miR-29a-3p, and shRNAs against FEM1B and GLI1.

Cell viability assay

Cells viability was measured with indicated conditions in 96-well plates containing 100 μL of

RPMI1640 and 10% FBS. Treatment time was 48 h before 100 µL of CellTiter-Glo® Reagent was added and the plate shaken on a plate shaker for 2 min to mix the reagent. Cells were then incubated at room temperature for 10 min to obtain steady state luminescent signals, which was detected on BioTek Synergy HT Microplate Reader. The Y-axis is labelled as "cell viability" and refers to the relative number of cells after 48 h incubation. The number of cells without oxaliplatin was set to 100% and used for normalization. A minimum of 3 independent experiments were used to calculate means and standard deviations.

Cell death assay

Cell death induced by oxaliplatin was determined in LoVo and OR cells using the CellTox™Green Cytotoxicity assay (Promega) according to manufacturer's suggestions. Briefly, LoVo and OR cells were grown in 96-well plates, in a mixture of cell culture medium and CellTox™Green Dye (1:1000). Cells were treated with oxaliplatin from 0 to 75 µM. Cell death was determined after 48 h of treatment by measuring the fluorescence intensity (485/520 nm excitation/emission) with a microplate reader. This assay measures membrane integrity. The CellTox™Green is excluded from viable cells, but enters dead cells to bind DNA, which significantly increases fluorescence of the dye. The Y-axis is labelled as "cell death fold" and refers to the increase in cell death (fluorescence) observed upon treatment with oxaliplatin after 48 h. Fluorescence of untreated cells after 48 h incubation was set to "1" for normalization. A minimum of 3 independent experiments were used to calculate means and standard deviations.

qPCR

RNA was isolated using Quick-RNA™ MiniPrep Kit (ZYMO RESEARCH, Bentley Cir Tustin, CA) according to manufacturer's protocol. First-strand cDNA for gene expression analysis was obtained from 5 µg of RNA using random primers and the PrimeScriptTM 1st strand cDNA Synthesis Kit (TAKARA, Mountain View, CA) according to manufacturer's instructions. Samples for quantitative reverse transcription real-time PCR (qPCR) were prepared using the iQTM SYBR® Green qPCR kit from Finnzymes (Bio-Rad Laboratories, Hercules, CA). Reaction mixes contained 10 µL of master mix, 1 µL of a 6X dilution of cDNA and 10 µM of amplification primers in a total reaction volume of 20 µL. GAPDH was used as a constant reference gene. The qPCR reactions were performed with iQTM SYBR® Green supermix System (Bio-Rad Laboratories, Hercules, CA). Each run was completed with a melting curve analysis to confirm the specificity of amplification and lack of primer dimers. Calculations were performed using Genex MacroTM version 1.1 software (Bio-Rad Laboratories, Hercules, CA).

Wound healing/scratch assay

Cells were grown in RPMI1640 and 10% FBS in six-well plates. Confluent monolayers were scratched with a 10 µL sterile micropipette tip, washed with PBS to remove floating cells, incubated in serum-free medium for 4 h, and finally move back to serum-containing growth medium. The number of cells in the scratched area were counted 0, 24 and 48 h after scratching.

Xenograft studies

Eight-week-old nude mice were obtained from BioLASCO. Mice weighing between 25-32 g were randomly allocated into 10 groups with 3 mice in each group and 2 tumors each mouse: $1*10^6$ LoVo or OR-LoVo cells were subcutaneously injected into nude mice. After a week the tumors reached an average volume of 80 mm^3, 10 nmol of miRNA negative control (miR01102-1-1, RiboBio, China), mimic (5'-UAGCACCAUCUGAAAUCGGUUA-3'), and inhibitor (5'-UAACCGAUUUCAGAUGGUGCUA-3') (RiboBio, China) were directly injected in tumors every 3 days as indicated. In addition, 1.6 mg/kg of oxaliplatin was injected itraperitoneal every 3 days after miRNA injection. The body weight of the mice was assessed throughout the experiment. The tumor volumes were calculated based on measurements (width^2 × length)/2 [14]. The mice were sacrificed using carbon dioxide overdose 5 weeks after cell injection. All experimental procedures and protocols were approved by the Institutional Animal Care and Use Committee (IACUC), based on institutional and national guidelines for the care and use of animals. One-way ANOVA has been used in multiple sets of comparison analyses. Statistically significant changes are shown (*P < 0.05, **P < 0.01, and ***P < 0.001).

Histological analysis

Tumors were washed in 1X PBS, and then fixed in 10% formalin for 12 h. The prepared tissue samples were immersed in PBS for 30 min followed by 0.85% NaCl for another 30 min. Samples were soaked in different concentrations of EtOH (70%, 85%, 95% and 100%) for 15, 30, 30 and 30 min, respectively. This process was repeated twice to dehydrate samples. The dehydrated tissue samples were embedded by the following procedure. Samples were soaked in 100% xylene twice for 30 min, and then in a solution of xylene and paraffin (v/v=1/1) for 45 min at 60°C. Finally, samples were incubated in 100% paraffin three times for 20 min at 60°C. Embedded samples were cut to sections (0.5 μm thickness). FEM1B and GLI1 staining was performed on 10 μm sections using antibodies from Abcam and Santa Cruz (Cambridge, UK and TX, USA) incubate at 4°C overnight. The tumor tissue samples were then stained with R.T.U. VECTASTAIN® Anti-Mouse IgG/Rabbit IgG/Goat IgG (Vector Laboratories, Cat. No. PK-7800) and ImmPACT™ DAB Peroxidase Substrate (Vector Laboratories, Cat. No. SK-4105) for 20 min according to the manufacturer's instructions.

Tissue grinding and cell lysis

The collected tissue from LoVo and OR-LoVo tumor groups tumors were washed in PBS buffer and about 0.1 g tissue was extracted in 1 mL lysis buffer (20 mM Tris, 2 mM EDTA, 50 mM 2-mercaptoethanol, 10% glycerol, Protease inhibitor, Phosphatase inhibitor). The mixture was homogenized for 20 min, 1200 r.p.m. at 4°C in a homogenizer stand with support rod.

Western blotting

Protein samples in 1X loading dye (50 mM Tris-HCl pH 6.8, 2% SDS, 10% glycerol, 1% β-mercaptoethanol, 12.5 mM EDTA, 0.02% bromophenol blue) were boiled for 10 min and separated by SDS-PAGE, before transfer to a PVDF membrane by semi-dry blotting. The PVDF membrane was blocked in 5% non-fat milk TBST (Tris-buffered saline Tween-20), incubated with the respective antibodies in TBST/5% milk, washed, and incubated with secondary antibodies conjugated to peroxidase. Antibody signals were developed as follows: anti-FEM1B, anti-GLI1 and anti-β-actin (Santa Cruz Biotechnology, Dallas, TX, USA). Anti-C-Caspase-3 (Cell Signaling Technology, Danvers, MA, USA).

Analyses of DNA damage by immunofluorescence

Cells were grown in RPMI1640 and 10% FBS in six-well plates on cover slips with 15 μM oxaliplatin overnight 37°C. Cells were then incubated in pre-extraction buffer (10 mM PIPES at pH 6.8, 100 mM $NaCl_2$, 300 mM sucrose, 0.2% Triton X-100) for 5 min at 4°C, before fixation using 4% paraformaldehyde, 3% Sucrose in 1X PBS for 20 min. Cold methanol (-20°C) was added to complete fixation for 10 min at -20°C. Samples were incubated in 2 mL of blocking buffer (2%, BSA and 10% milk in 1X PBS-T) for 30 min. Cells were then incubated with primary antibody diluted in 1X PBS-T containing 2% BSA and 10% milk at room temperature for 2 h. Coverslips were washed three times with PBS-T before 1 h incubation with the appropriate secondary antibodies conjugated to fluorophores (Cy3 or Alexa-488). After three washes with PBS-T, cells were stained with DAPI. Images were captured using a Leica DMi8 THUNDER microscope. For the quantitative fluorescence analysis of individual cells, pictures of cells were randomly selected and the level of γH2AX signal in individual cells was quantify inside of the DAPI area.

Measurement of intracellular platinum concentrations by ICP-MS

LoVo and OR-LoVo cells were grown to 90% confluency in 10 cm dishes. Cells were harvested using trypsin, and $7.5*10^5$ cells were seeded into each well of the 6-well plate and cultured in 2.5 ml medium at 37°C in 5% CO_2. On the next day cells were treated with 15 or 45 μM oxaliplatin in RPMI 1640 medium at 37°C for 0, 60, 120, and 240 min. The medium was removed and cells washed twice in ice-cold PBS before plates were placed on ice. 215 μl nitric acid (70%) was added to each well, and samples incubated overnight at room temperature. The following day the nitric acid extracted solution was transferred into Omni-vials and incubated at 65°C overnight to dissolve cellular debris. Nitric acid was then diluted with 3 ml of buffer (0.1% Triton X-100, 1.4% nitric acid, 1 ppb in H_2O) and incubate again at 65°C overnight. A ThermoiCAPRQ C2 ICP-MS system was used to

measure the platinum (Pt) element. A Pt standard (500 ppt, 1 ppb, 2 ppb, 5 ppb, 10 ppb) was used for quantitation of signals.

Survey of gene expression in TCGA

TCGA Colorectal Cancer (COAD) data was accessed via UCSC Xena (https://xena.ucsc.edu/) on August 2, 2022 and used for downstream analyses. While no annotations for MIR29A-3p were observed among the updated counts matrix, remapping of the transcript from raw bam files identified potential overlapping reads for the transcript (ENSG00000284032) with an overlapping long non-coding RNA (LINC00513). Therefore, in these analyses, the expression of LINC00513 was used as a surrogate for MIR29A-3p levels. Tumor vs surrounding tissue annotations were extracted using TCGA barcode IDs, where only tumor expression of LINC00513/MIR29A-3p was used for survival curves and differential expression analyses. Expression categories (high or low) for MIR29A-3p and FEM1B were assigned based on relative levels of each gene compared to the population means. All data was analyzed using R open source software, where correlations performed from the biweight midcorrelation coefficient and corresponding regression pvalue (ref: https://doi.org/10.1186/1471-2105-9-559) Survival curves and analyses were using R packages 'survival' and 'survminer'. Differential expression was performed using limma and pathway enrichments analyzed via WebGestalt (ref: https://doi.org/10.1093/nar/gkx356).

Statistical analysis

The experimental data are shown by mean ± S.E.M.

Results

miR-29a-3p confers oxaliplatin resistance in cancer cells

We have previously selected oxaliplatin resistant OR-LoVo cells by growing LoVo cells in oxaliplatin containing growth media [1]. OR-LoVo cells are significantly more resistant to oxaliplatin as compared to LoVo cells with the IC_{50} changing from about 15 μM to over 60 μM (**Figure 1A**). In addition, oxaliplatin induced cell death was dramatically reduced in OR-LoVo cells (**Figure 1B**). MicroRNA array profiling identified a few microRNAs with differential expression in LoVo and OR-LoVo cells [1]. We selected miR-29a-3p for further evaluation because its expression was significantly elevated in tumors compared to matched surrounding tissue (**Figure 1C**). Consistent with miR-29a-3p conferring oxaliplatin resistance, miR-29a-3p was barely detectable in parental LoVo cells, but expressed at significant levels in OR-LoVo cells as detected by qPCR (**Figure 1D**). We next asked whether miR-29a-3p expression is sufficient to confer oxaliplatin resistance. Ectopic expression of miR-29a-3p in LoVo cells resulted in dramatically increased tolerance to oxaliplatin and resistance reached the level observed in OR-LoVo cells (**Figure 1E**). In contrast, expression of miR-29a-3p in OR-LoVo cells resulted in only a subtle additional increase in resistance (**Figure 1E**). These results suggest that miR-29a-3p expression is sufficient to induce drug tolerance and is a major contributor to oxaliplatin resistance in OR-LoVo cells. A similar induction of resistance to oxaliplatin was also observed in other cancer cell lines, such as HeLa and ovarian cancer cells TOV-112D (**Figure 1F**). In contrast, oxaliplatin sensitivity of the two breast cancer cell lines tested, MDA-MB468 and MCF7, was either unaffected or very modestly suppressed by expression of miR-29a-3p (**Figure 1F**). Similarly, oxaliplatin sensitivity of the K-RAS^{G13D} expressing colon cancer cell line HCT116 was not altered by miR-29a-3p expression (**Figure 1F**). These results demonstrate that miR-29a-3p expression can induce resistance to oxaliplatin in a variety of cancer cells with different tissue origin and is not restricted to colon cancer.

Regulation of Fem1B by miR-29a-3p induces oxaliplatin resistance

To identify miR-29a-3p targets that mediate oxaliplatin resistance, we used the miBase tool [15]. One of the predicted targets, the VHL-box protein Fem1B, caught our attention, because it has previously been linked to regulation of apoptosis in colon cancer [16]. Specifically, Fem1b has pro-apoptotic properties, and was proposed to interact with apoptosis-inducing proteins Fas, tumor necrosis factor receptor-1 (TNFR1), and apoptotic protease activating factor-1 (Apaf-1) to activate downstream apoptosis pathways [7, 8]. Consistent with miR-29a-3p

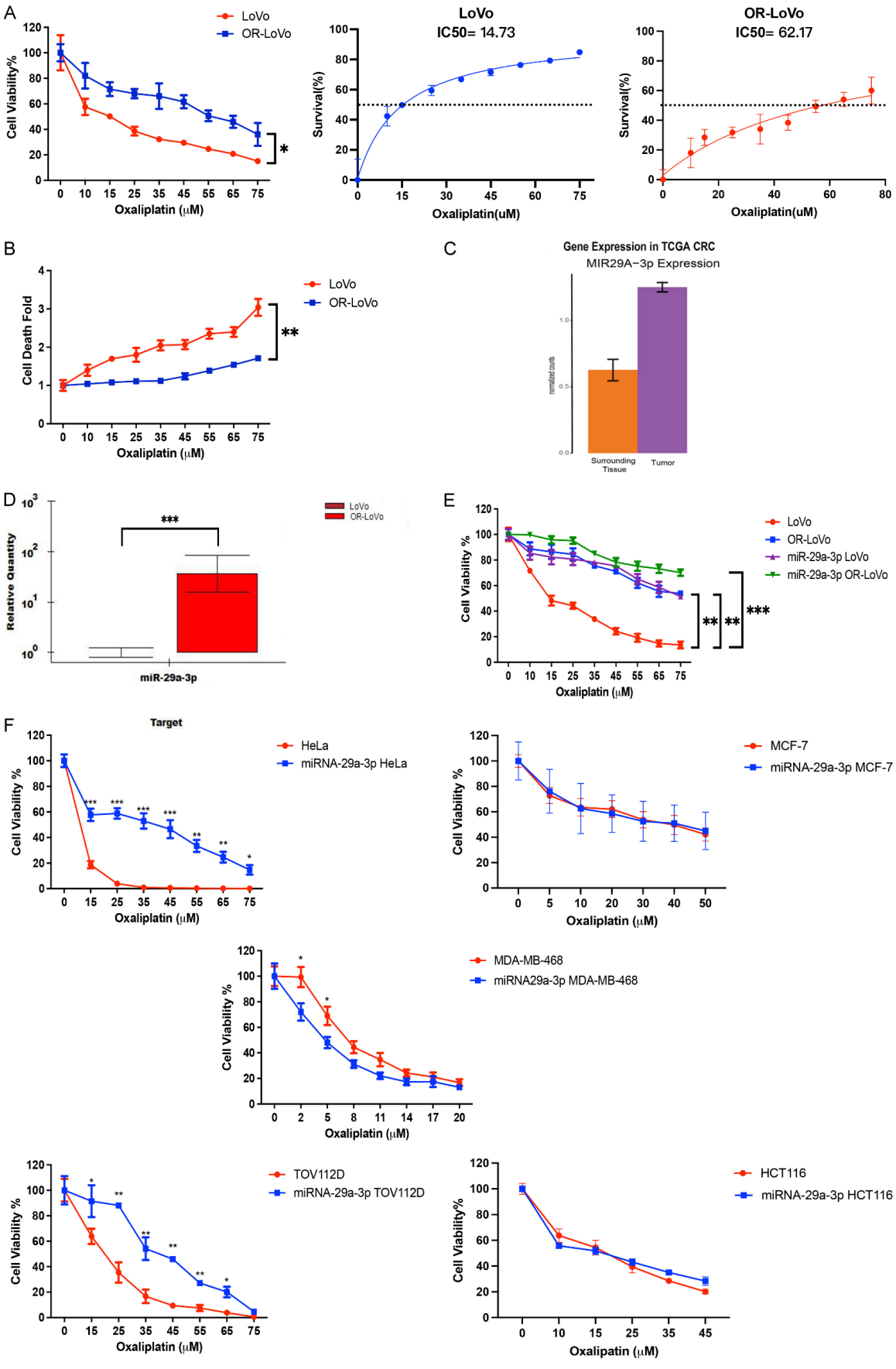
A
LoVo
OR-LoVo
Cell Viability%
Oxaliplatin (μM)
*
LoVo
IC50= 14.73
Survival(%)
Oxaliplatin(uM)
OR-LoVo
IC50= 62.17
Survival(%)
Oxaliplatin(uM)
B
LoVo
OR-LoVo
Cell Death Fold
Oxaliplatin (μM)
**
C
Gene Expression in TCGA CRC
MIR29A−3p Expression
normalized counts
Surrounding Tissue
Tumor
D
LoVo
OR-LoVo
Relative Quantity
***
miR-29a-3p
E
LoVo
OR-LoVo
miR-29a-3p LoVo
miR-29a-3p OR-LoVo
Cell Viability %
Oxaliplatin (μM)
**
**
***
F
Target
HeLa
miRNA-29a-3p HeLa
Cell Viability %
Oxaliplatin (μM)
MCF-7
miRNA-29a-3p MCF-7
Cell Viability %
Oxaliplatin (μM)
MDA-MB-468
miRNA29a-3p MDA-MB-468
Cell Viability %
Oxaliplatin (μM)
TOV112D
miRNA-29a-3p TOV112D
Cell Viability %
Oxaliplatin (μM)
HCT116
miRNA-29a-3p HCT116
Cell Viability%
Oxalipatin (μM)

Figure 1. miRNA-29a-3p confers oxaliplatin resistance to LoVo cells. (A) LoVo and OR-LoVo cells were treated with different concentrations of oxaliplatin and cell numbers were quantified with the CellTiter-Glo assay after 48 h. Right panels: IC_{50} determination. (B) As (A), but cell viability was analyzed using the CellTox assay. (C) Relative expression of mir29a-3p (see methods) in colorectal carcinoma patients from TCGA in tumor (n=329) or matched patient surrounding tissue (n=49). (D) miRNA 29a-3p specifically detected by qPCR in OR-LoVo cells but barely detectable in parental LoVo cells. (E) LoVo and OR-LoVo cells exogenously expressing miRNA-29a-3p were analyzed as in (A). (F) Oxaliplatin sensitivity of HeLa, TOV-112D, MDA-MB-468, MCF7, and HCT116 cells with or without ectopic expression of miRNA-29a-3p was analyzed as in (A).

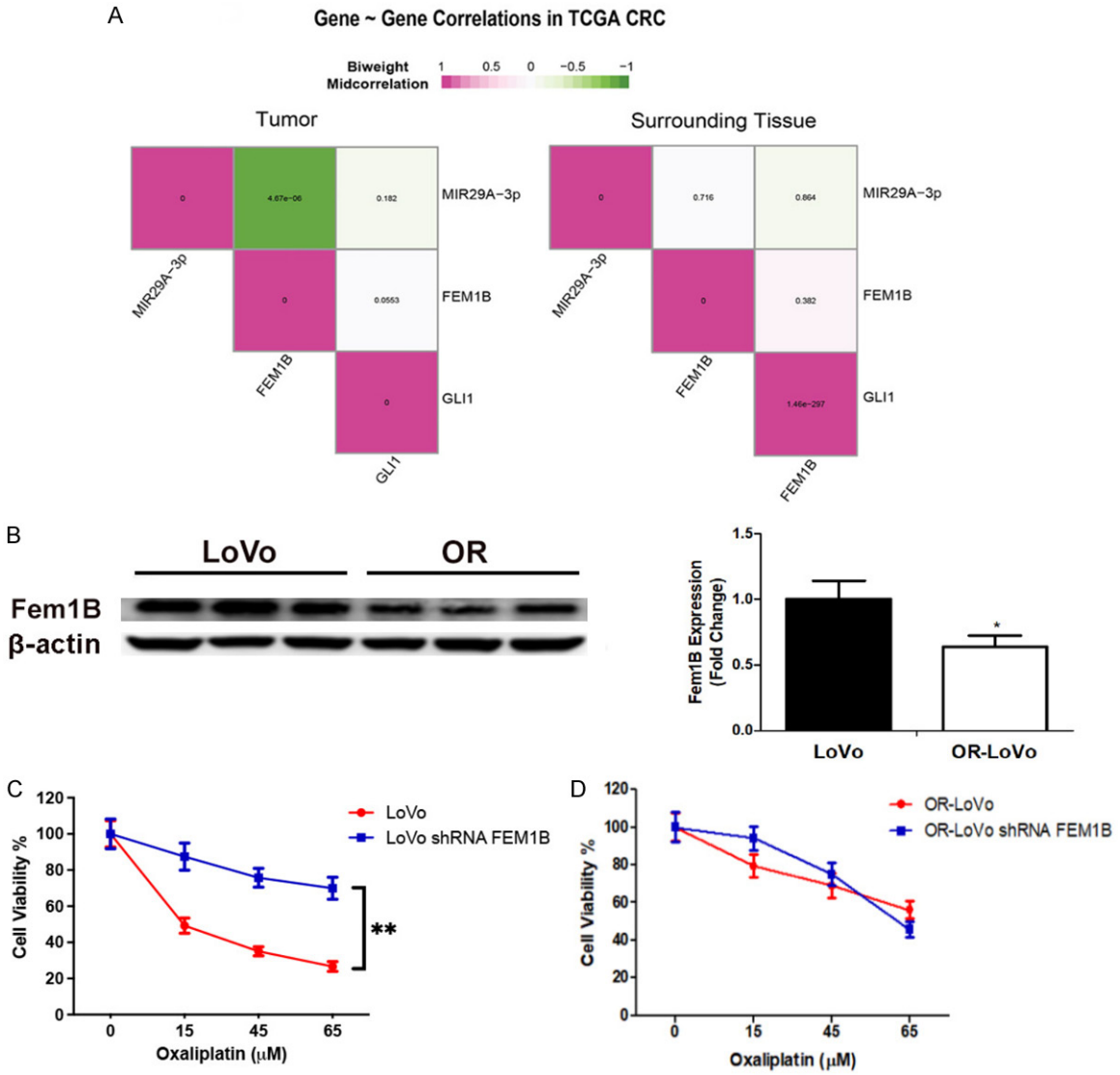

Figure 2. Changes in Fem1B levels correlate with oxaliplatin resistance. (A) Correlation structure between relevant genes mir29A-3p, FEM1B, and GLI1 in the same samples, where color indicates regression coefficient and filled values show corresponding p-statistics. (B) Fem1B protein levels were determined by Western blotting. Three biological replicates are shown, which were quantified on the right. (C, D) FEM1B and GLI1 were knocked down in LoVo (C) or OR-LoVo cells (D) using stable expression of shRNAs. Cells were then treated with oxaliplatin and cell numbers determined using CellTiter-Glo. Successful knockdown of Fem1B was verified as shown in **Figure 3A**.

regulating Fem1B we observed a strong negative correlation with FEM1B expression only in tumors, where no significant relationship was observed in surrounding tissue (**Figure 2A**). No significant correlation was however observed with expression of GLI1, a major target of

Fem1B, possibly due to the predominantly post-translational nature of Gli1 regulation by Fem1B (**Figure 2A**). Consistent with miR-29a target predictions, Fem1B protein levels were significantly lower in OR-LoVo cells as compared to the oxaliplatin sensitive parental cell line (**Figure 2B**). These results suggested that miR-29a-3p may confer oxaliplatin resistance by downregulation of Fem1B protein levels. This hypothesis predicts that, like increasing miR-29a-3p expression, downregulation of FEM1B using shRNA should increase oxaliplatin tolerance in LoVo cell. Consistent with this hypothesis, LoVo cells stably expressing shRNAs against FEM1B were significantly more resistant to oxaliplatin than the parental cells (**Figure 2C**). In contrast, expression of shRNAs targeting FEM1B in OR-LoVo cells, which already have reduced Fem1B, had only a subtle effect on oxaliplatin sensitivity (**Figure 2D**). These results demonstrate that Fem1B downregulation through miR-29a-3p can induce resistance to oxaliplatin.

Misregulation of the Fem1B ubiquitylation target Gli1 confers chemoresistance

Fem1B is a substrate recognition subunit of the Cul2-ubiquitin ligase and has been shown to target the Glioma-Associated Oncogene Homolog 1 (Gli1) for degradation by the 26S proteasome [17]. Accordingly, downregulation of FEM1B by shRNA expression increased GLI1 levels (**Figure 3A**). Conversely, overexpression of FEM1B reduced Gli1 steady state levels (**Figure 3B**). Furthermore, the increased Fem1b levels also induced an apoptotic program as indicated by cleaved Cas3 (**Figure 3B**), which is consistent with previous studies that described Fem1B as a proapoptotic protein that regulates apoptosis in colon cancer cells [7, 8]. We hypothesized that high levels of miR-29a-3p in OR-LoVo cells downregulated Fem1b resulting in elevated Gli1 levels. Reducing Gli1 levels in OR-LoVo cells should therefore reverse oxaliplatin resistance in these cells. Indeed, shRNA based GLI1 knockdown significantly decreased oxaliplatin sensitivity of OR-LoVo cells (**Figure 3C**), but had no effect on the parental LoVo cells (**Figure 3D**). Consistent with these results, in vitro wound healing assays demonstrated increased proliferation potential of OR-LoVo cells as compared to parental LoVo cells, which was reversed by knockdown of Gli1 (**Figure 3E** and **3F**). These results suggest that Gli1 confers chemoresistance in OR-LoVo cells.

Chemoresistant OR-LoVo cells have reduced DNA damage accumulation

The repair process of oxaliplatin induced DNA damage involves generation of DNA double-strand brakes [18]. One of the first steps during DNA double strand brake repair is the phosphorylation of the histone variant H2AX at damage sites to form γ-H2AX, which in turn initiates recruitment of repair proteins [19, 20]. The extent of DNA damage can thus be visualized by quantitation of γ-H2AX foci [21]. LoVo cells showed strong γ-H2AX staining when cells were treated with as little as 15 μM oxaliplatin for 48 hours (**Figure 4A**). In contrast, OR-LoVo cells required much higher dose of oxaliplatin to develop phospho-γH2AX marked repair foci (**Figure 4A**). A time course of γH2AX staining comparing the dynamics of repair foci development after treatment with 15 μM oxaliplatin confirmed rapid induction of DNA damage in LoVo cells, but very little DNA damage in resistant OR-LoVo cells (**Figure 4B**). This defect is specific for oxaliplatin treatment, because etoposide or H_2O_2 treatment caused a similar induction of DNA damage in LoVo and OR-LoVo cells (**Figure 4A** and **4C**).

OR-LoVo cells have reduced intracellular oxaliplatin concentrations and higher capacity to repair oxaliplatin damage

OR-LoVo cells show a striking resistance to oxaliplatin, which is also reflected by the low level of DNA damage these cells experience upon oxaliplatin treatment (**Figure 4**). A possible explanation for the resistance to oxaliplatin is that OR-LoVo cells can reduce the intracellular drug concentration by either blocking uptake or increasing efflux. We therefore measured the intracellular concentration of platinum by inductively coupled plasma mass spectrometry (ICP-MS). Cells were treated with either 15 μM or 45 μM oxaliplatin and intracellular platinum was measured 0, 60, and 240 min after drug exposure (**Figure 5A**, **5B**). OR-LoVo cells showed modestly, but significantly reduced intracellular platinum concentrations as compared to LoVo cells. However, comparing intracellular platinum concentrations with biological effects suggest that additional mechanisms must contribute to oxaliplatin resistance of OR-LoVo cells.

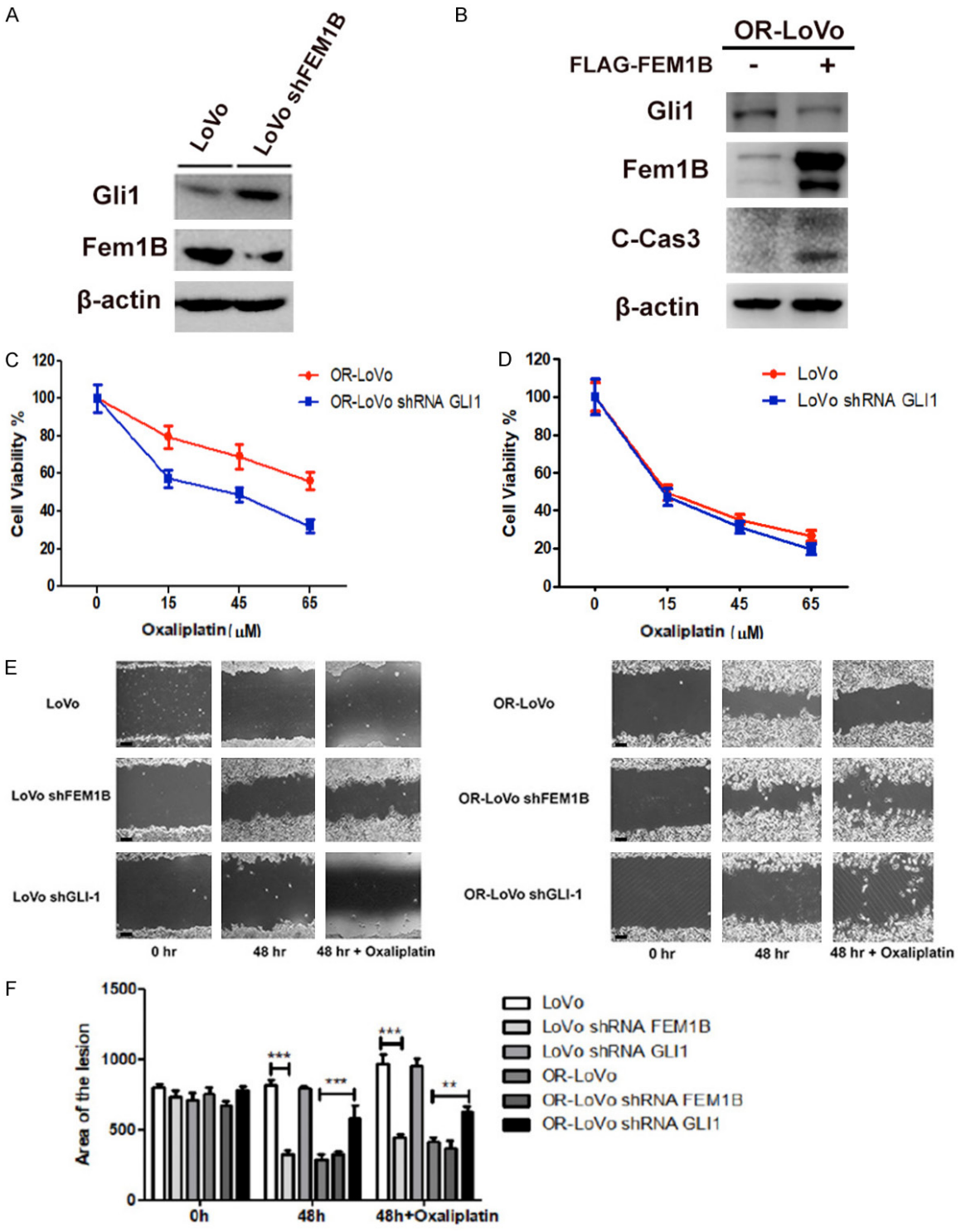

Figure 3. Gli1 confers chemoresistance in OR-LoVo cells. (A) LoVo cells treated with shRNA-FEM1B resulted in up-regulation of Gli1 levels as determined by Western blotting. (B) OR-LoVo cells were transfected with FLAG-FEM1B to overexpress FEM1B, which resulted in reduced Gli1 levels as determined by Western blotting. (C, D) Gli1 was knocked-down in OR-LoVo (C) and LoVo cells (D) and sensitivity to oxaliplatin was analyzed using CellTiter-Glo. (E) Wound healing assay was performed from 0 to 48 h. Scale bar: 20 μm. (F) The quantitation was determined by measuring the area of the lesion.

The IC_{50} of LoVo cells for oxaliplatin is about 15 μM compared to > 60 μM for OR-LoVo cells (**Figure 1**). We measured about 4 ppb of platinum in LoVo cells after treatment with 15 μM

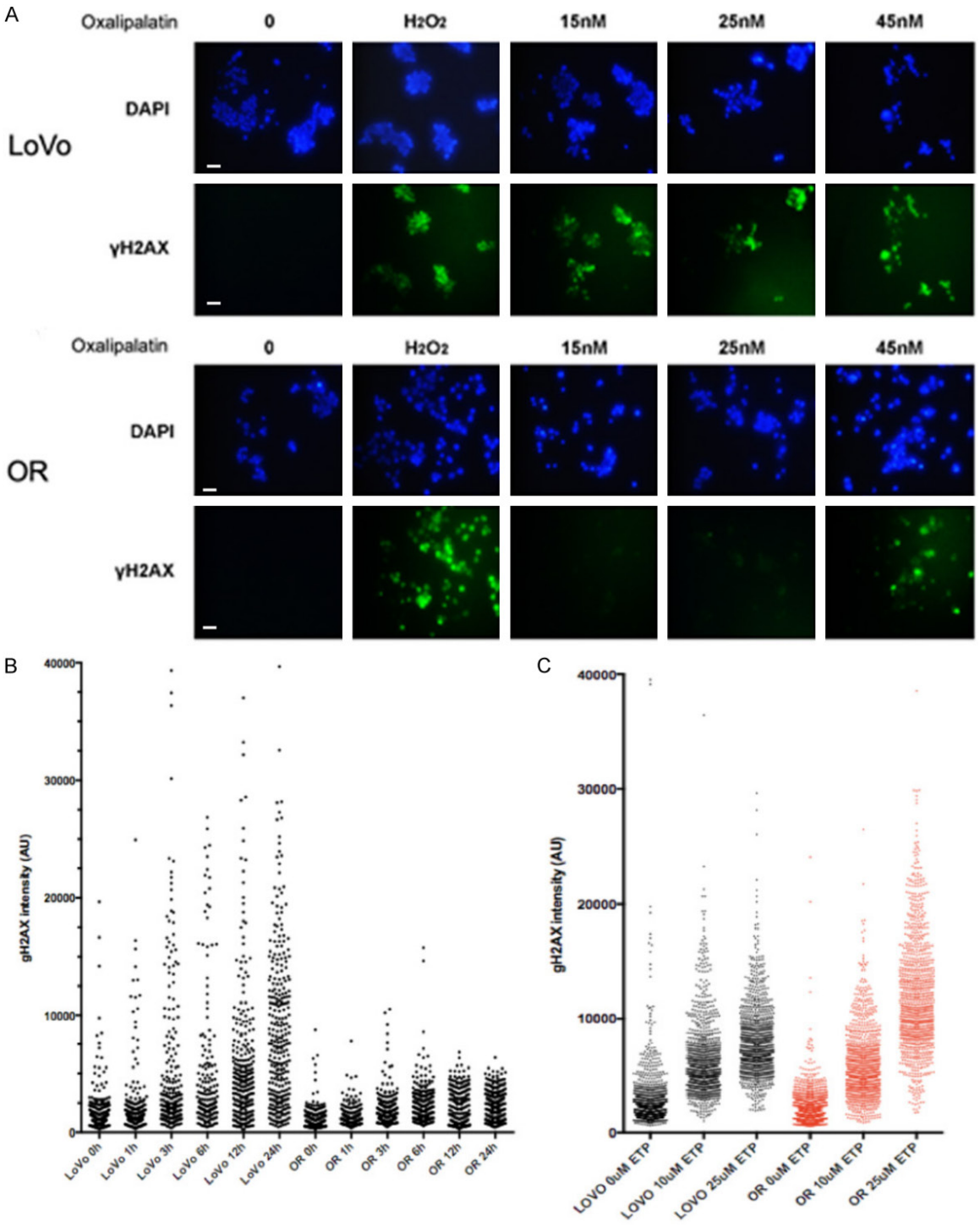

Figure 4. Chemoresistant OR-LoVo cells have reduced DNA damage accumulation. A. γ-H2AX foci were determined by immunofluorescence following treatment with oxaliplatin at the indicated concentration. Scale bar: 20 μm. B. The level of γ-H2AX intensity was quantified in 300 cells after oxaliplatin treatment from 0 to 24 h in LoVo and OR-LoVo cells. C. The intensity of γ-H2AX staining was quantified in 1000 cells after treatment with etoposide for 1 h.

oxaliplatin, a concentration that correlates with the IC_{50} for these cells. OR-LoVo cells treated with 45 μM of oxaliplatin contain about 10 ppb of intracellular platinum, an intracellular concentration more than twice as high as the concentration that kills 50% of LoVo cells. Yet, over

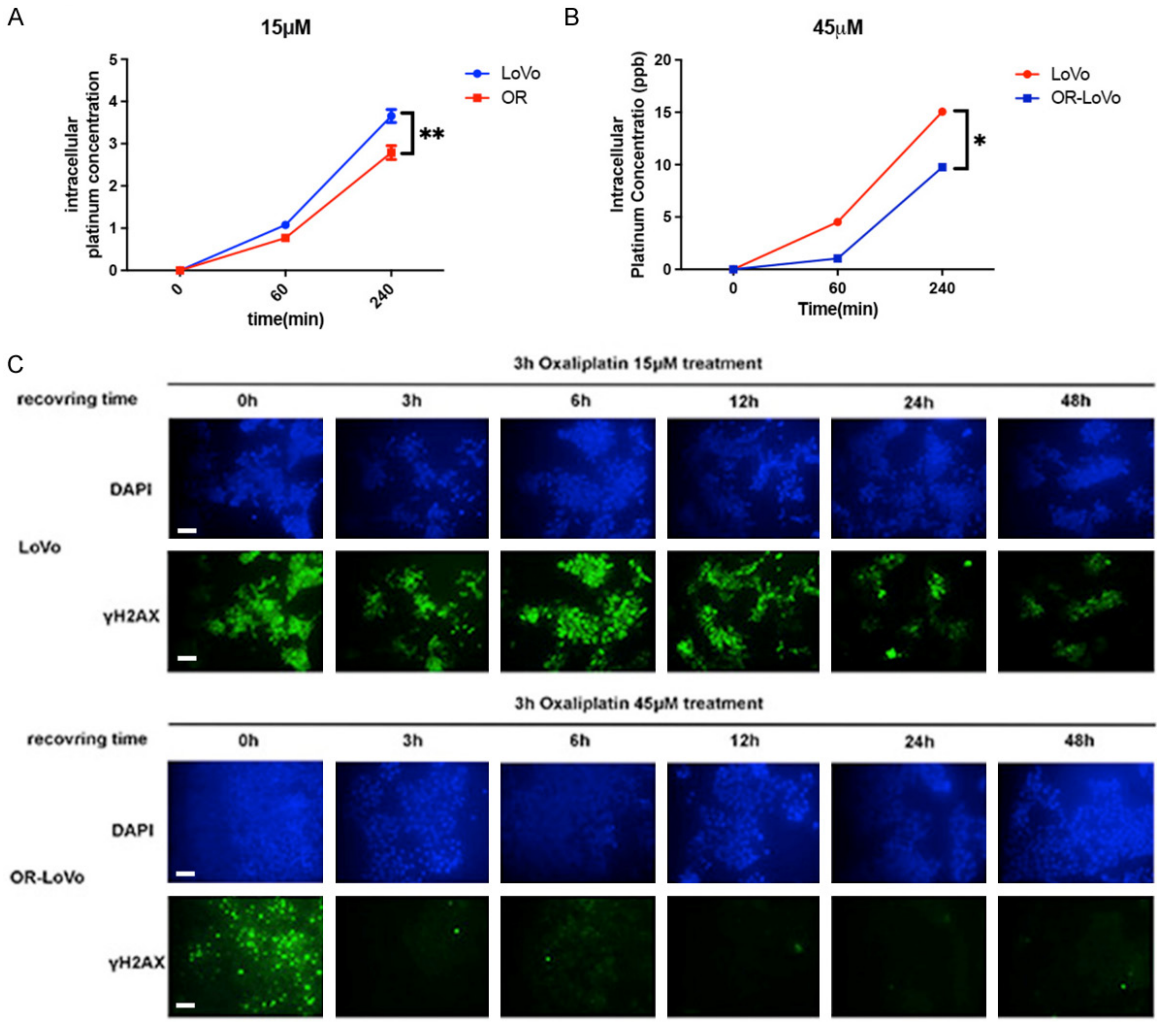

Figure 5. Reduced oxaliplatin uptake and increased recovery from oxaliplatin-induce damage in OR-LoVo cells. (A, B) Intracellular platinum concentrations were determined by ICP-MS in LoVo and OR-LoVo cells after treatment with 15 μM (A) or 45 μM of oxaliplatin (B). (C) Recovery from oxaliplatin-induced damage was determined by γ-H2AX staining after treatment with 15 μM (LoVo cells) or 45 μM (OR-LoVo cells) oxaliplatin for 3 h over a time period from 0 to 48 h after oxaliplatin was removed. Scale bar: 20 μm.

70% of OR-LoVo cells survive these oxaliplatin concentrations (**Figures 1** and **5**). While there is a significant reduction in oxaliplatin uptake/efflux, it can only partially explain the reduced DNA damage observed in OR-LoVo cells. We therefore monitored recovery of cells from oxaliplatin damage to assess repair capacity (**Figure 5C**). Cells were treated for 3 h with 15 μM (LoVo cells) or 45 μM (OR-LoVo cells) oxaliplatin to induce DNA damage, which was monitored through γ-H2AX foci. The higher dose for OR-LoVo cells was necessary because 15 μM oxaliplatin does not induce robust γ-H2AX foci in the resistant cells (**Figure 4A**). Oxaliplatin was then removed and γ-H2AX foci were followed over time. OR-LoVo cells recovered much more rapidly than parental LoVo cells suggesting that OR-LoVo cells also acquired a more efficient repair process to eliminate DNA damage induce by oxaliplatin.

miR-29a-3p mediates oxaliplatin resistance in colon cancer xenografts

Oxaliplatin chemotherapy is a first-line treatment for metastatic colorectal cancers. We were therefore interested whether miR-29a-3p expression affects therapeutic outcomes in xenograft models. We generated subcutaneous tumors by injection of LoVo and OR-LoVo cells. The tumors maintained the characteristics we have determined in cell culture such

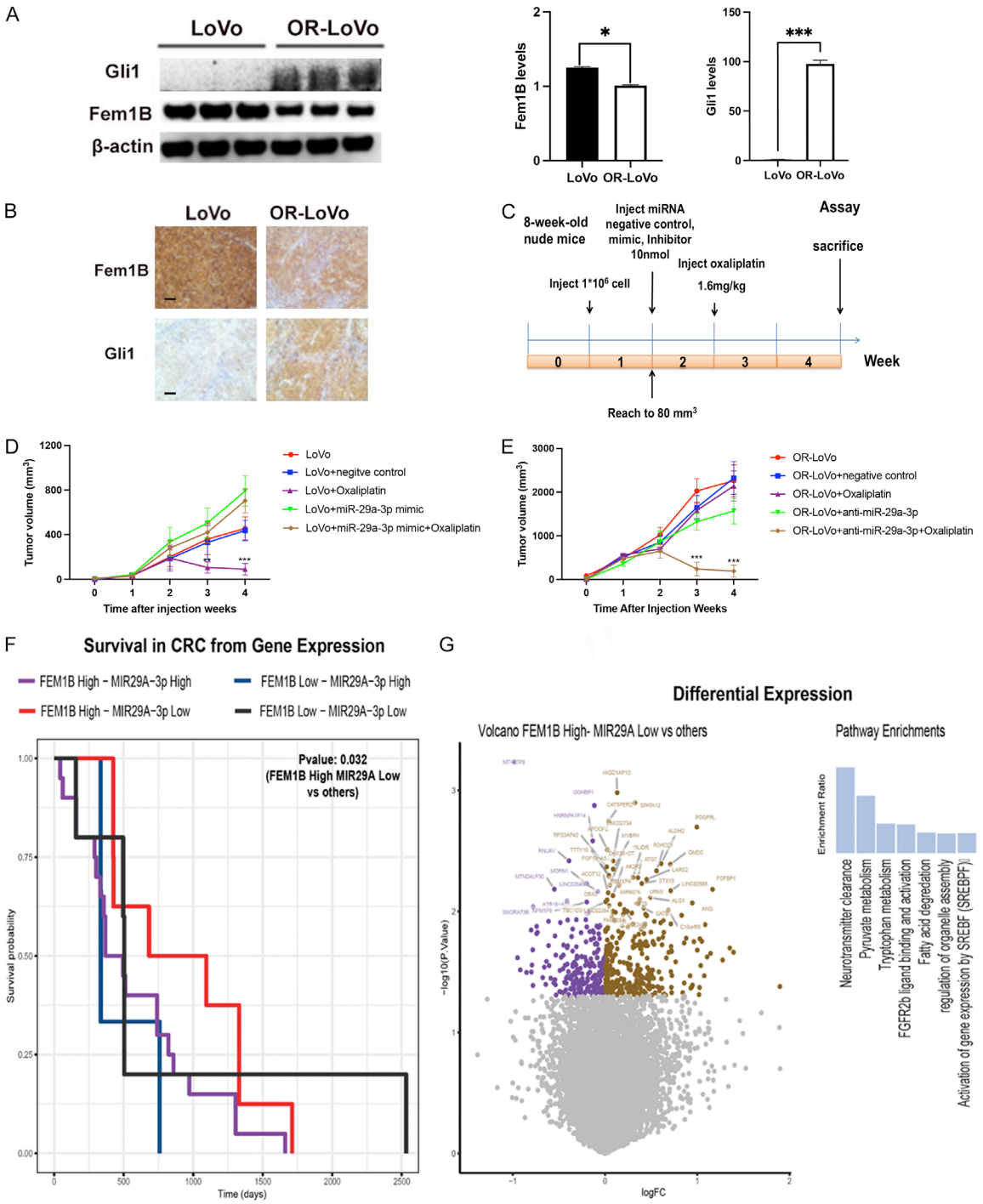

Figure 6. miRNA-29a-3p mediates oxaliplatin resistance in colon cancer xenografts. (A, B) Gli1 and Fem1B levels were determine in three tumors by Western blotting (A, quantitation on the right) or immunohistochemistry (B) in xenografts generated in nude mice. Scale bar: 20 μm. (C) Experimental design for xenograft assays and treatment. (D) The tumor growth of LoVo cell xenografted in nude mice in five different groups. Treatment was administered every 3 days from week 1 to 4. (E) The tumor growth of OR-LoVo cell xenografted in five different groups as in (D). (F) Patient survival curves among all groups corresponding to high or low mir29A-3p and/or FEM1B expression. *P*-value quantified using log-rank method comparing FEM1B-high mir29A low individuals to all others. (G) Differential gene expression in tumors comparing FEM1B High/mir29A low individuals to all others, plotted as a volcano (left) and corresponding pathway enrichments (right).

that LoVo tumors had very low Gli1 expression but higher Fem1B levels as compared to OR-LoVo cells (**Figure 6A** and **6B**). For experiments with LoVo tumors, one week after subcu-

taneous administration of cells, miR-29a-3p was injected into the tumors and mice were treated with oxaliplatin in week 2 (**Figure 6C**). Similar to our observations in cell culture, evaluation of tumor size demonstrated that expression of miR-29a-3p significantly reduced the tumor response to oxaliplatin treatment (**Figure 6D**). Consistent with these findings, tumors generated with the oxaliplatin resistant OR-LoVo cell lines, which naturally express high levels of miR-29a-3p, were resistant to oxaliplatin treatment. However, when anti-miR-29a-3p was injected into the forming tumor, oxaliplatin induced complete regression, confirming that miR-29a-3p plays an important role in oxaliplatin resistance in vivo (**Figure 6E**).

Conservation of miR-29a-3p mechanism in TCGA

To define which aspects of this novel mechanism of miR-29a-3p action persisted in available human datasets, TCGA COAD data (ref: https://doi.org/10.1038/nature11252) was analyzed for patterns of concordance with cell culture and mouse model data. To assess if the interaction between miR-29a-3p and FEM1B we discovered in this study showed relevant trends in patient data, patients were binned into groups based on expression (low or high) of the two genes. Here, patients with high FEM1B and low miR29a-3p showed significantly better survival when compared to the 3 other groups based on expression categories (**Figure 6F**), where those with low FEM1B and high miR29a-3p showed reduced survival. Next, differential expression was performed on all genes between high FEM1B/low miR29a-3p expressing individuals compared to all others (**Figure 6G**). Pathway analyses of these genes suggested various amino acid and lipid metabolism pathways, as well as growth factor signaling as differing the most between the two groups. Collectively, these analyses show that the interaction between mir29a-3p and FEM1B and consequent disease relevance is conserved in human TCGA data.

Discussion

Colorectal cancer is among the most common cancers and contributes significantly to cancer related deaths in the world. Oxaliplatin is widely used for the treatment of colorectal carcinoma [22, 23]. Like other platinum-based therapeutics, oxaliplatin induces DNA crosslinks, which prevent DNA replication and ultimately induce cell death [24, 25]. Drug resistance is a common problem in cancer therapy and aberrant miRNA expression has been linked to occurrence of oxaliplatin resistance [26, 27]. However, mechanisms of oxaliplatin resistance have not been described. Here we used the LoVo colorectal cancer cell model with a derived oxaliplatin resistant line, OR-LoVo, to gain mechanistic insight into the causes of oxaliplatin resistance. We found that the expression level of miR-29-3p correlates with resistance, and that expression of this miRNA is sufficient to induce resistance to oxaliplatin in cells as well as animal tumor models. Furthermore, downregulation of miR-29a-3p in oxaliplatin resistant cells reverts cells and tumors to the drug sensitive phenotype of the parental LoVo cells. We further demonstrated that the pro-apoptotic ubiquitin ligase component Fem1b and the transcription factor Gli1 are likely regulated by miR-29a-3p to modulate drug resistance. Cell culture experiments demonstrated that reducing Fem1b levels using shRNA in LoVo cells mimics the effect of miR-29a-3p expression to induce drug resistance. Conversely, knockdown of Gli1 expression in drug resistant OR-LoVo cells induced oxaliplatin sensitivity. These results suggest a model whereby miR-29a-3p reduces Fem1b expression, which in turn attenuates Gli1 degradation resulting in oxaliplatin resistance.

Oxaliplatin resistance has been linked to miRNA expression previously. miR-27b, miR-148a, and miR-326 were significantly increased in plasma from patients with metastatic colorectal cancers with poor therapy response [28]. However, no functional studies were done to confirmed a direct effect beyond this correlation. In contrast, functional evidence exists for other miRNAs. miR-153 was shown to provide resistance to oxaliplatin in SW480 colon cancer cells [29], and miR-203 overexpression increased resistance of HT29 cells [30]. Effects of miR-153 and miR-203 were relatively modest compared to the dramatically increased oxaliplatin tolerance we report here for miR-29a-3p. Resistance to platinum compounds, including oxaliplatin, can be induced by (a) reduced intracellular drug concentrations due to increased drug efflux or decreased uptake, (b) more efficient repair of platinum induced DNA lesions, and (c) effective

detoxification [5]. The latter does not seem to play a major role in therapy resistance in the clinic. We found that OR-LoVo cells have a significantly decreased intracellular platinum concentration as compared to LoVo cells, suggesting enhanced oxaliplatin efflux and/or reduced uptake. However, the reduction in intracellular oxaliplatin concentration is not sufficient to explain the significant oxaliplatin tolerance of OR-LoVo cells. Changes in repair capacity likely plays an additional role in the resistance mechanism. We did observe a rapid loss of γ-H2AX foci in OR-LoVo cells after removal of oxaliplatin. In contrast, LoVo cells showed a much slower recovery, indicating that repair potential of oxaliplatin-induced DNA lesions may be increased in OR-LoVo cells.

In summary, our study highlights the importance of miRNAs in therapy resistance in cancer and supports the possibility that miR-29a-3p plays important roles in resistance of colorectal cancers to the first-line therapeutic oxaliplatin by controlling Fem1b and Gli1 levels.

Acknowledgements

This work was funded by National Institute of Health grant R35 GM148350-01 to P.K.

Disclosure of conflict of interest

None.

Address correspondence to: Chih-Yang Huang, Graduate Institute of Basic Medical Science, China Medical University, Taichung 404, Taiwan. Tel: +886-0922-772-329; E-mail: cyhuang@mail.cmu.edu.tw; Peter Kaiser, Department of Biological Chemistry, University of California, Irvine, California 92697, USA. Tel: 1-949-824-9367; E-mail: pkaiser@uci.edu

References

[1] Hsu HH, Kuo WW, Shih HN, Cheng SF, Yang CK, Chen MC, Tu CC, Viswanadha VP, Liao PH and Huang CY. FOXC1 regulation of miR-31-5p confers oxaliplatin resistance by targeting LATS2 in colorectal cancer. Cancers (Basel) 2019; 11: 1576.

[2] Kelland L. The resurgence of platinum-based cancer chemotherapy. Nat Rev Cancer 2007; 7: 573-584.

[3] Muggia FM and Fojo T. Platinums: extending their therapeutic spectrum. J Chemother 2004; 16 Suppl 4: 77-82.

[4] Graham J, Mushin M and Kirkpatrick P. Oxaliplatin. Nat Rev Drug Discov 2004; 3: 11-12.

[5] Martinez-Balibrea E, Martinez-Cardus A, Gines A, Ruiz de Porras V, Moutinho C, Layos L, Manzano JL, Buges C, Bystrup S, Esteller M and Abad A. Tumor-related molecular mechanisms of oxaliplatin resistance. Mol Cancer Ther 2015; 14: 1767-1776.

[6] Dankert JF, Pagan JK, Starostina NG, Kipreos ET and Pagano M. FEM1 proteins are ancient regulators of SLBP degradation. Cell Cycle 2017; 16: 556-564.

[7] Subauste MC, Sansom OJ, Porecha N, Raich N, Du L and Maher JF. Fem1b, a proapoptotic protein, mediates proteasome inhibitor-induced apoptosis of human colon cancer cells. Mol Carcinog 2010; 49: 105-113.

[8] Subauste MC, Ventura-Holman T, Du L, Subauste JS, Chan SL, Yu VC and Maher JF. RACK1 downregulates levels of the pro-apoptotic protein Fem1b in apoptosis-resistant colon cancer cells. Cancer Biol Ther 2009; 8: 2297-2305.

[9] Manford AG, Mena EL, Shih KY, Gee CL, McMinimy R, Martinez-Gonzalez B, Sherriff R, Lew B, Zoltek M, Rodriguez-Perez F, Woldesenbet M, Kuriyan J and Rape M. Structural basis and regulation of the reductive stress response. Cell 2021; 184: 5375-5390, e5316.

[10] Manford AG, Rodriguez-Perez F, Shih KY, Shi Z, Berdan CA, Choe M, Titov DV, Nomura DK and Rape M. A cellular mechanism to detect and alleviate reductive stress. Cell 2020; 183: 46-61, e21.

[11] Sanjana NE, Shalem O and Zhang F. Improved vectors and genome-wide libraries for CRISPR screening. Nat Methods 2014; 11: 783-784.

[12] Joung J, Konermann S, Gootenberg JS, Abudayyeh OO, Platt RJ, Brigham MD, Sanjana NE and Zhang F. Genome-scale CRISPR-Cas9 knockout and transcriptional activation screening. Nat Protoc 2017; 12: 828-863.

[13] Shin KJ, Wall EA, Zavzavadjian JR, Santat LA, Liu J, Hwang JI, Rebres R, Roach T, Seaman W, Simon MI and Fraser ID. A single lentiviral vector platform for microRNA-based conditional RNA interference and coordinated transgene expression. Proc Natl Acad Sci U S A 2006; 103: 13759-13764.

[14] Faustino-Rocha A, Oliveira PA, Pinho-Oliveira J, Teixeira-Guedes C, Soares-Maia R, da Costa RG, Colaco B, Pires MJ, Colaco J, Ferreira R and Ginja M. Estimation of rat mammary tumor volume using caliper and ultrasonography measurements. Lab Anim (NY) 2013; 42: 217-224.

[15] Griffiths-Jones S, Saini HK, van Dongen S and Enright AJ. miRBase: tools for microRNA ge-

nomics. Nucleic Acids Res 2008; 36: D154-D158.
[16] Kamura T, Maenaka K, Kotoshiba S, Matsumoto M, Kohda D, Conaway RC, Conaway JW and Nakayama KI. VHL-box and SOCS-box domains determine binding specificity for Cul2-Rbx1 and Cul5-Rbx2 modules of ubiquitin ligases. Genes Dev 2004; 18: 3055-3065.
[17] Gilder AS, Chen YB, Jackson RJ 3rd, Jiang J and Maher JF. Fem1b promotes ubiquitylation and suppresses transcriptional activity of Gli1. Biochem Biophys Res Commun 2013; 440: 431-436.
[18] Bakkenist CJ, Lee JJ and Schmitz JC. ATM is required for the repair of oxaliplatin-induced DNA damage in colorectal cancer. Clin Colorectal Cancer 2018; 17: 255-257.
[19] Brand M, Sommer M, Ellmann S, Wuest W, May MS, Eller A, Vogt S, Lell MM, Kuefner MA and Uder M. Influence of different antioxidants on X-ray induced DNA Double-Strand Breaks (DSBs) using gamma-H2AX immunofluorescence microscopy in a preliminary study. PLoS One 2015; 10: e0127142.
[20] Ivashkevich A, Redon CE, Nakamura AJ, Martin RF and Martin OA. Use of the gamma-H2AX assay to monitor DNA damage and repair in translational cancer research. Cancer Lett 2012; 327: 123-133.
[21] Mah LJ, El-Osta A and Karagiannis TC. gammaH2AX: a sensitive molecular marker of DNA damage and repair. Leukemia 2010; 24: 679-686.
[22] Kim GP, Sargent DJ, Mahoney MR, Rowland KM Jr, Philip PA, Mitchell E, Mathews AP, Fitch TR, Goldberg RM, Alberts SR and Pitot HC. Phase III noninferiority trial comparing irinotecan with oxaliplatin, fluorouracil, and leucovorin in patients with advanced colorectal carcinoma previously treated with fluorouracil: N9841. J Clin Oncol 2009; 27: 2848-2854.
[23] Nehls O, Porschen R, Gregor M and Klump B. The role of oxaliplatin in the therapy for advanced colorectal carcinoma. Z Gastroenterol 2001; 39: 1033-1047.
[24] Alcindor T and Beauger N. Oxaliplatin: a review in the era of molecularly targeted therapy. Curr Oncol 2011; 18: 18-25.
[25] Kim NR and Kim YJ. Oxaliplatin regulates myeloid-derived suppressor cell-mediated immunosuppression via downregulation of nuclear factor-kappaB signaling. Cancer Med 2019; 8: 276-288.
[26] Hua Y, Zhu Y, Zhang J, Zhu Z, Ning Z, Chen H, Liu L, Chen Z and Meng Z. miR-122 targets X-linked inhibitor of apoptosis protein to sensitize oxaliplatin-resistant colorectal cancer cells to oxaliplatin-mediated cytotoxicity. Cell Physiol Biochem 2018; 51: 2148-2159.
[27] Ren WW, Li DD, Chen X, Li XL, He YP, Guo LH, Liu LN, Sun LP and Zhang XP. MicroRNA-125b reverses oxaliplatin resistance in hepatocellular carcinoma by negatively regulating EVA1A mediated autophagy. Cell Death Dis 2018; 9: 547.
[28] Kjersem JB, Ikdahl T, Lingjaerde OC, Guren T, Tveit KM and Kure EH. Plasma microRNAs predicting clinical outcome in metastatic colorectal cancer patients receiving first-line oxaliplatin-based treatment. Mol Oncol 2014; 8: 59-67.
[29] Zhang L, Pickard K, Jenei V, Bullock MD, Bruce A, Mitter R, Kelly G, Paraskeva C, Strefford J, Primrose J, Thomas GJ, Packham G and Mirnezami AH. miR-153 supports colorectal cancer progression via pleiotropic effects that enhance invasion and chemotherapeutic resistance. Cancer Res 2013; 73: 6435-6447.
[30] Zhou Y, Wan G, Spizzo R, Ivan C, Mathur R, Hu X, Ye X, Lu J, Fan F, Xia L, Calin GA, Ellis LM and Lu X. miR-203 induces oxaliplatin resistance in colorectal cancer cells by negatively regulating ATM kinase. Mol Oncol 2014; 8: 83-92.